Dual Effect of Coordination Field and Sulphuric Acid on Property of Single-Atom Catalyst in the Electrosynthesis of H_2O_2

Jinkong Pan[a], Qiaojun Fang[a], Qian Xia[b], Anfu Hu[b], Fuli Sun[a], Wei Zhang[a], Yifan Yu[a], Guilin Zhuang[a]*, Jian Jiang[b]*, Jianguo Wang[a]*

[a]Institute of Industrial Catalysis, State Key Laboratory Breeding Base of Green-Chemical Synthesis Technology, College of Chemical Engineering, Zhejiang University of Technology, Hangzhou 310032, P.R. China.

[b]China Tobacco Zhejiang Industrial Co., Ltd., Hangzhou 310032, P.R. China.

*Email: glzhuang@zjut.edu.cn (G. L. Zhuang), jiangj@zjtobacco.com (J. Jiang), jgw@zjut.edu.cn (J. g. Wang)

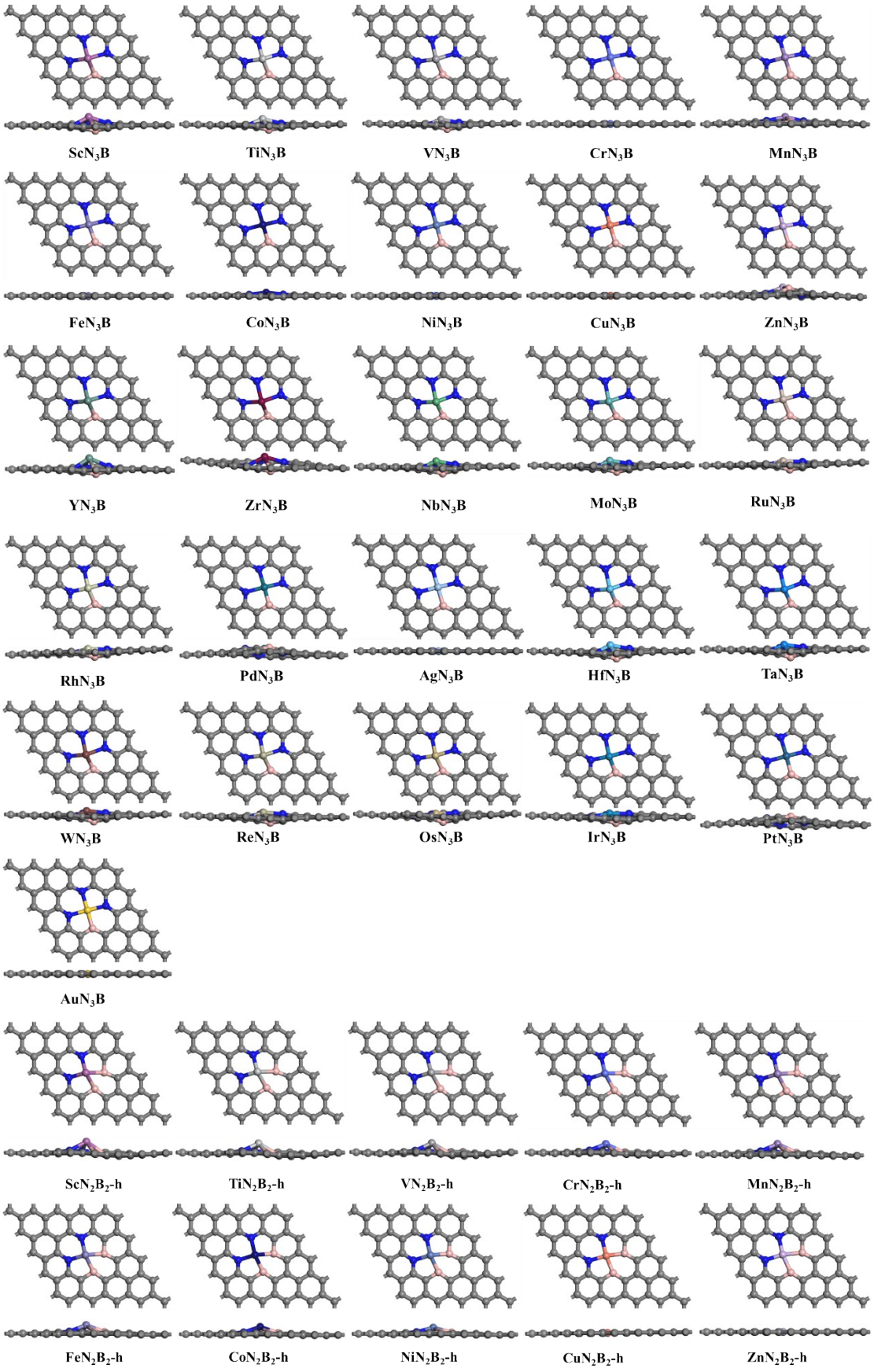
ScN3B
TiN3B
VN3B
CrN3B
MnN3B
FeN3B
CoN3B
NiN3B
CuN3B
ZnN3B
YN3B
ZrN3B
NbN3B
MoN3B
RuN3B
RhN3B
PdN3B
AgN3B
HfN3B
TaN3B
WN3B
ReN3B
OsN3B
IrN3B
PtN3B
AuN3B
ScN2B2-h
TiN2B2-h
VN2B2-h
CrN2B2-h
MnN2B2-h
FeN2B2-h
CoN2B2-h
NiN2B2-h
CuN2B2-h
ZnN2B2-h

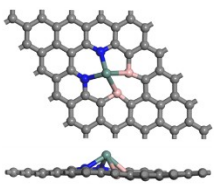

YN_2B_2-h

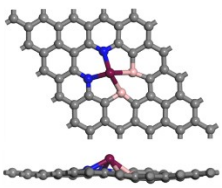

ZrN_2B_2-h

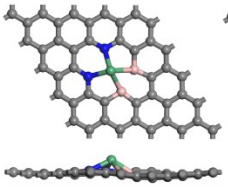

NbN_2B_2-h

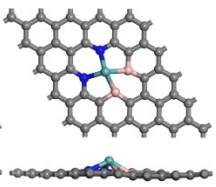

MoN_2B_2-h

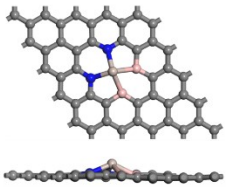

RuN_2B_2-h

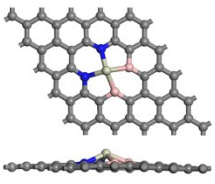

RhN_2B_2-h

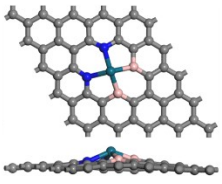

PdN_2B_2-h

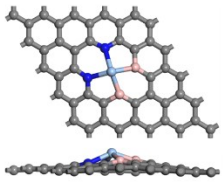

AgN_2B_2-h

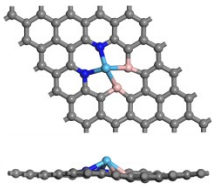

HfN_2B_2-h

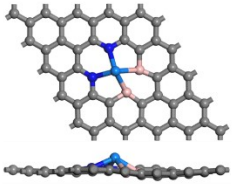

TaN_2B_2-h

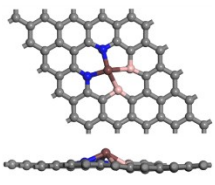

WN_2B_2-h

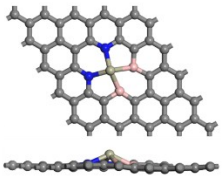

ReN_2B_2-h

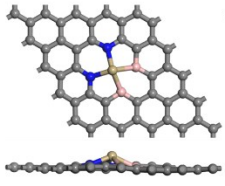

OsN_2B_2-h

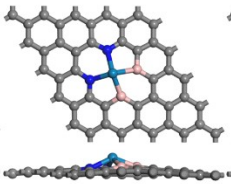

IrN_2B_2-h

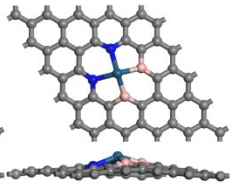

PtN_2B_2-h

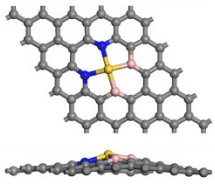

AuN_2B_2-h

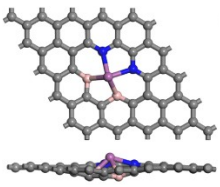

ScN_2B_2-p

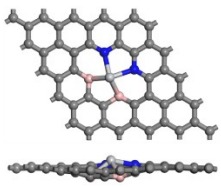

TiN_2B_2-p

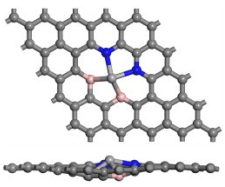

VN_2B_2-p

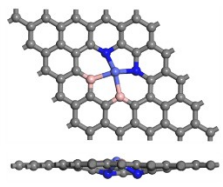

CrN_2B_2-p

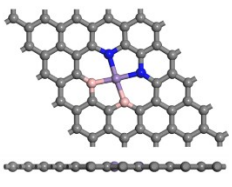

MnN_2B_2-p

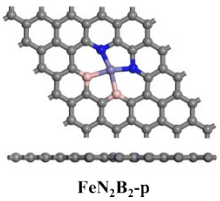

FeN_2B_2-p

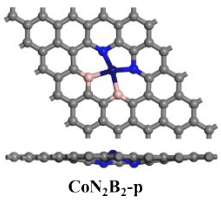

CoN_2B_2-p

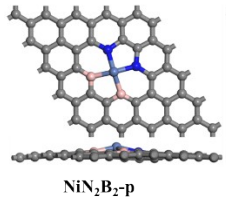

NiN_2B_2-p

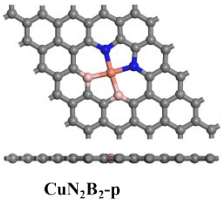

CuN_2B_2-p

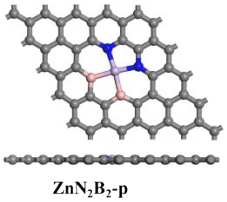

ZnN_2B_2-p

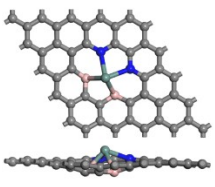

YN_2B_2-p

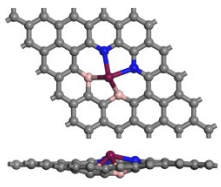

ZrN_2B_2-p

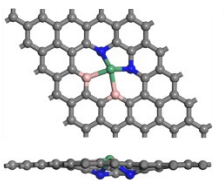

NbN_2B_2-p

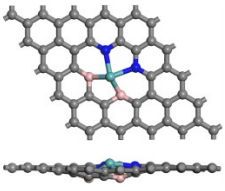

MoN_2B_2-p

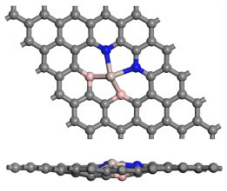

RuN_2B_2-p

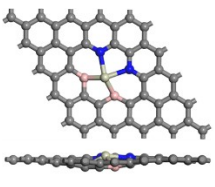

RhN_2B_2-p

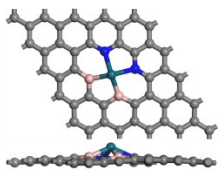

PdN_2B_2-p

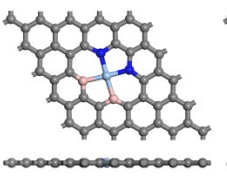

AgN_2B_2-p

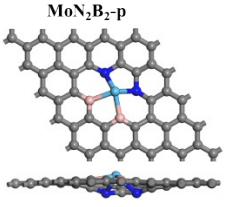

HfN_2B_2-p

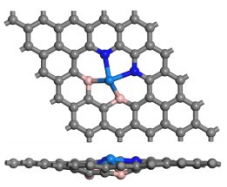

TaN_2B_2-p

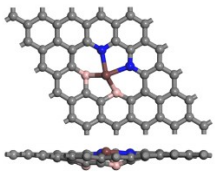

WN_2B_2-p

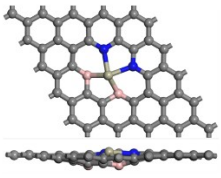

ReN_2B_2-p

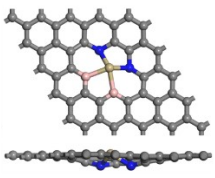

OsN_2B_2-p

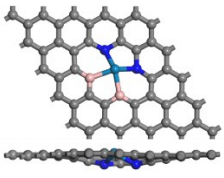

IrN_2B_2-p

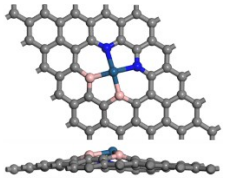

PtN_2B_2-p

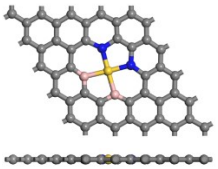

AuN_2B_2-p

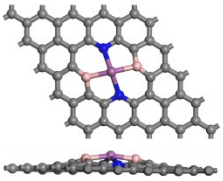

ScN_2B_2-o

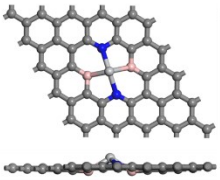

TiN_2B_2-o

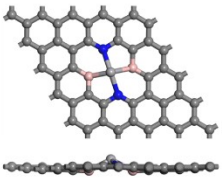

VN_2B_2-o

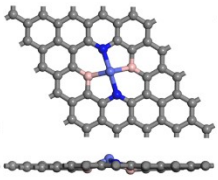

CrN_2B_2-o

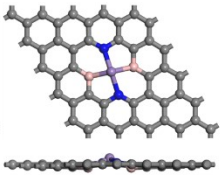

MnN_2B_2-o

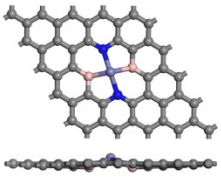

FeN_2B_2-o

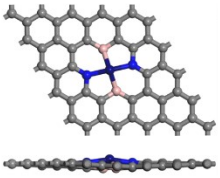

CoN_2B_2-o

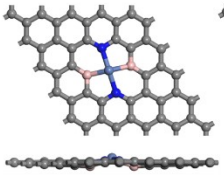

NiN_2B_2-o

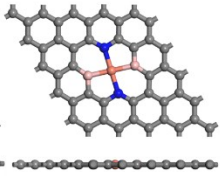

CuN_2B_2-o

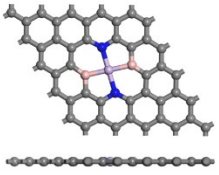

ZnN_2B_2-o

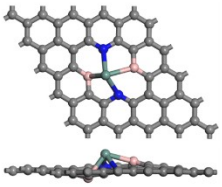

YN_2B_2-o

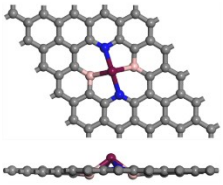

ZrN_2B_2-o

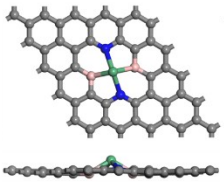

NbN_2B_2-o

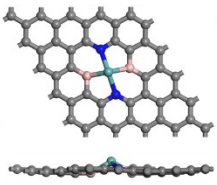

MoN_2B_2-o

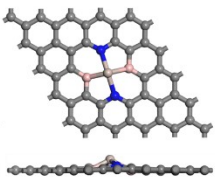

RuN_2B_2-o

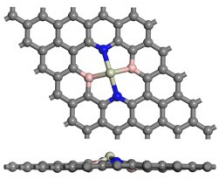

RhN_2B_2-o

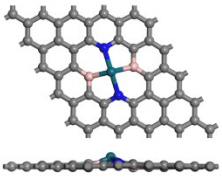

PdN_2B_2-o

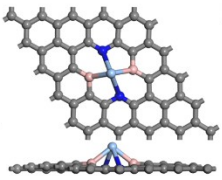

AgN_2B_2-o

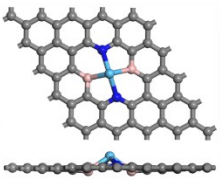

HfN_2B_2-o

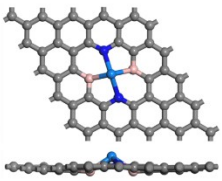

TaN_2B_2-o

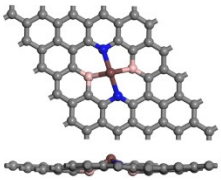

WN_2B_2-o

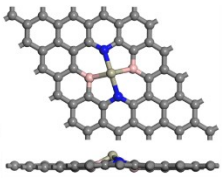

ReN_2B_2-o

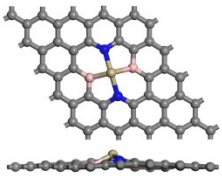

OsN_2B_2-o

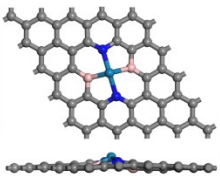

IrN_2B_2-o

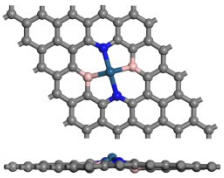

PtN_2B_2-o

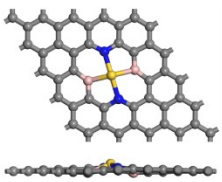

AuN_2B_2-o

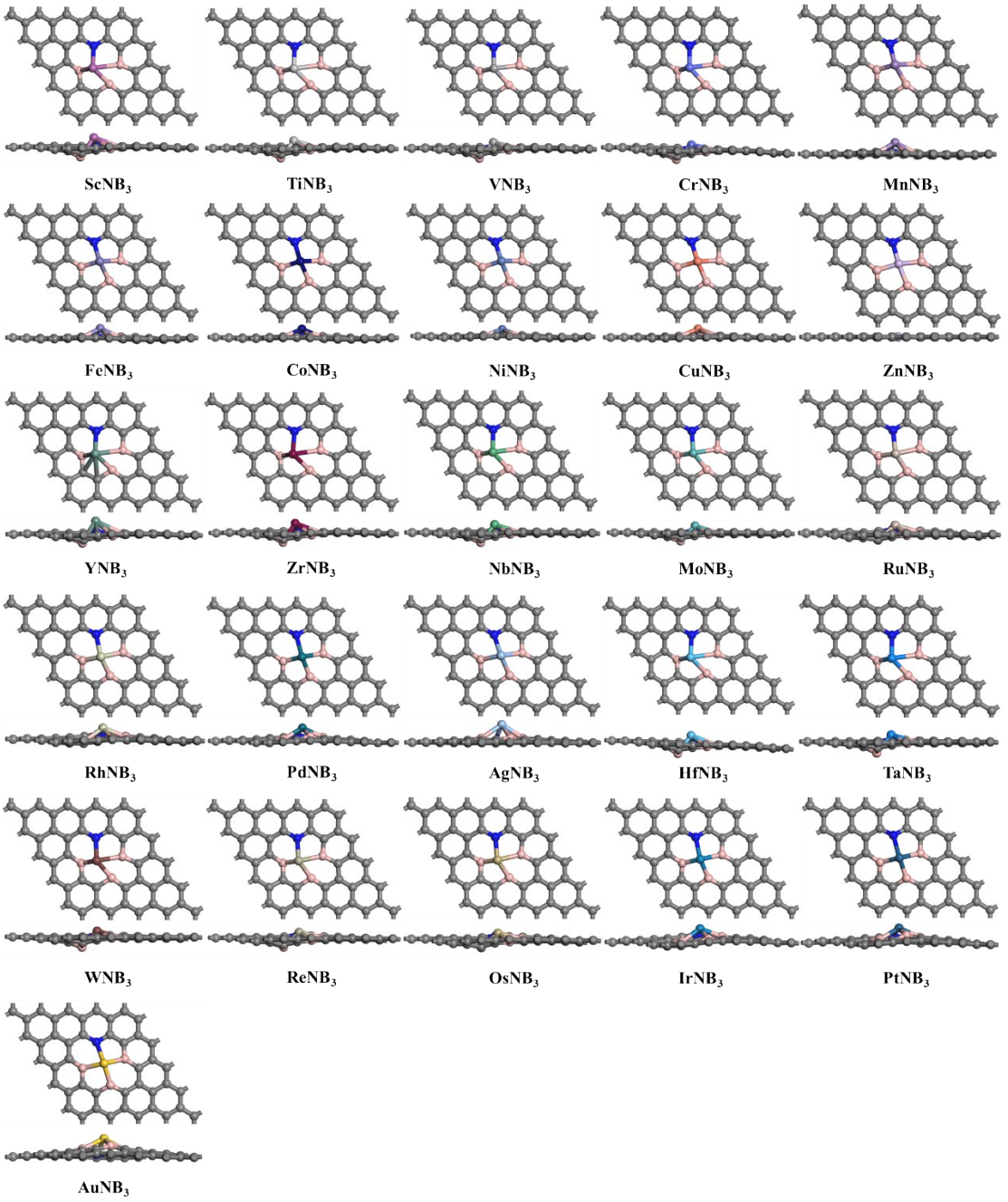
ScNB3
TiNB3
VNB3
CrNB3
MnNB3
FeNB3
CoNB3
NiNB3
CuNB3
ZnNB3
YNB3
ZrNB3
NbNB3
MoNB3
RuNB3
RhNB3
PdNB3
AgNB3
HfNB3
TaNB3
WNB3
ReNB3
OsNB3
IrNB3
PtNB3
AuNB3
ScB4
TiB4
VB4
CrB4
MnB4
FeB4
CoB4
NiB4
CuB4
ZnB4

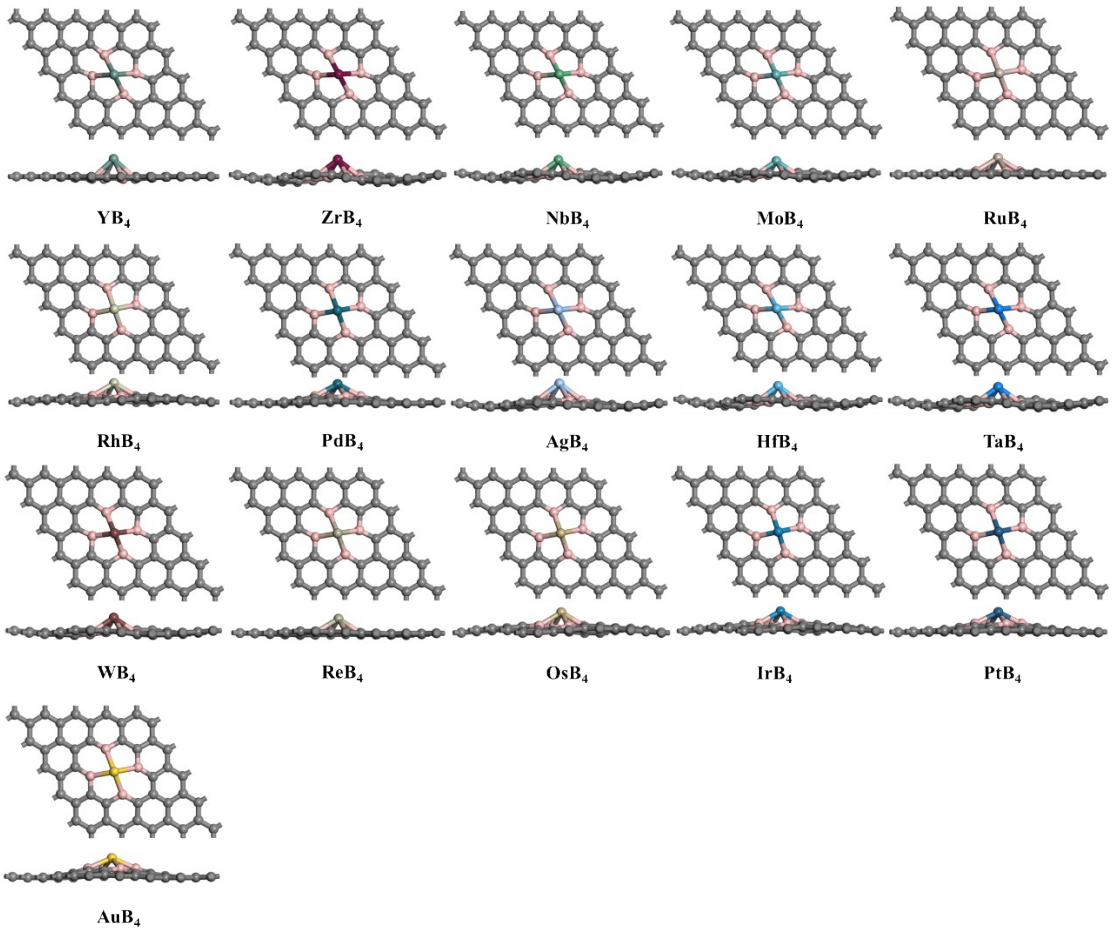

Fig. S1 Optimized structures of MN_3B, MN_2B_2-h, MN_2B_2-p, MN_2B_2-o, MNB_3, MB_4.

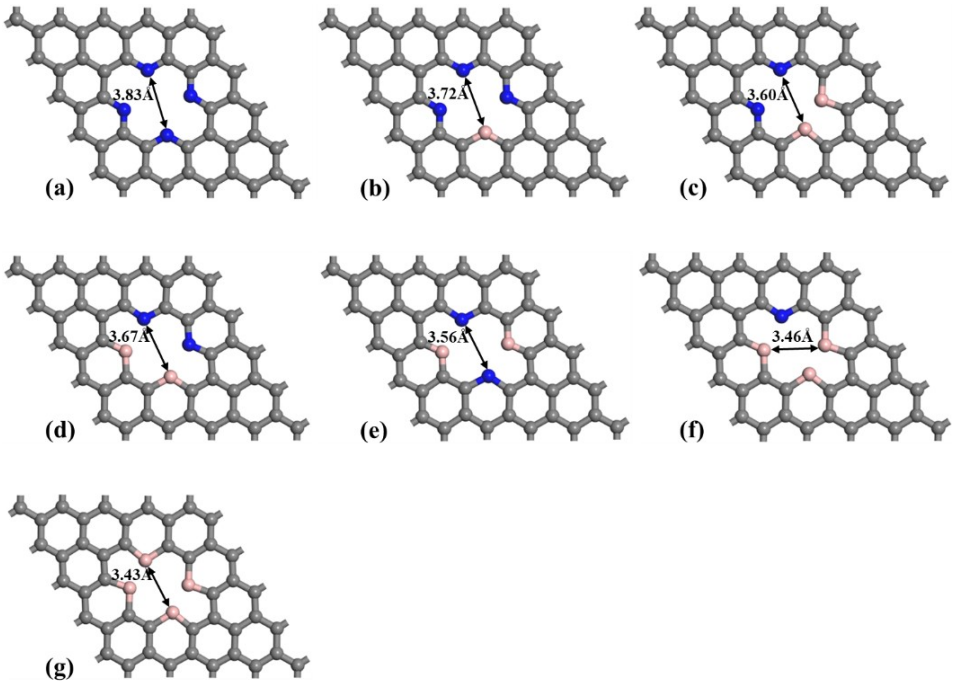

Fig. S2 Optimized structures of (a) V_N_4-gra, (b) V_N_3B-gra, (c) V_N_2B_2-h-gra, (d) V_N_2B_2-p-gra, (e) V_N_2B_2-p-gra, (f) V_NB_3-gra, (g) V_B_4-gra.

Table S1. Computed binding energies (E_b) for 26 single atoms embedded in each substrate. The thermodynamically unstable systems are highlighted by red color.

Metal	Binding Energy (E_b, eV)					
	MN_3B	MN_2B_2-h	MN_2B_2-p	MN_2B_2-o	MNB_3	MB_4
Sc	-2.13	-3.32	-0.54	0.18	-0.75	-0.79
Ti	-1.36	-1.99	0.15	0.56	0.15	0.51
V	-0.32	-0.74	1.39	0.99	0.96	1.10
Cr	0.13	-0.93	0.88	1.18	1.03	1.22
Mn	-1.06	-1.30	1.15	0.03	0.30	0.61
Fe	-0.48	-0.89	0.93	0.25	0.45	0.63
Co	-0.60	-0.90	0.36	0.19	0.24	0.37
Ni	-1.31	-1.15	0.13	-0.14	-0.20	-0.14
Cu	-0.90	-1.28	0.08	1.16	0.53	0.24
Zn	-0.54	-2.10	0.00	2.06	1.11	0.42
Y	-2.00	-3.31	-0.67	0.18	-0.74	-1.06
Zr	-1.37	-2.03	0.08	0.64	0.04	0.40
Nb	0.12	-0.37	0.88	1.21	1.31	1.53
Mo	1.09	0.53	1.56	1.67	1.95	1.94
Ru	0.77	-0.02	0.77	1.09	0.90	0.79
Rh	0.11	-0.14	0.21	0.05	0.12	-0.24
Pd	-0.17	-0.33	0.46	-0.05	0.00	-0.07
Ag	0.64	0.06	1.77	1.40	1.11	1.07
Hf	-1.17	-1.70	0.43	0.96	0.39	0.86
Ta	0.48	0.23	1.37	1.67	1.78	2.33
W	1.76	1.55	2.21	2.31	2.62	2.97
Re	2.26	1.20	1.94	2.17	2.17	2.26
Os	1.65	0.92	1.62	1.81	1.58	1.43
Ir	0.75	0.40	0.88	0.61	0.57	0.09
Pt	-0.18	-0.36	0.26	-0.12	-0.35	-0.48
Au	0.29	-0.48	0.90	1.65	0.57	0.40

Table S2. Adsorption configurations of O_2*, OOH*, and H_2O_2* on each thermodynamically stable system.

MN_3B	O_2*	OOH*	H_2O_2*
ScN_3B	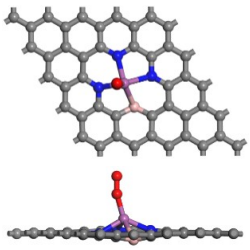	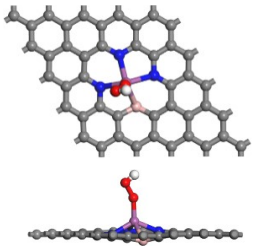	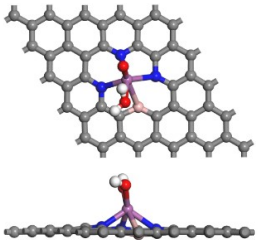
TiN_3B	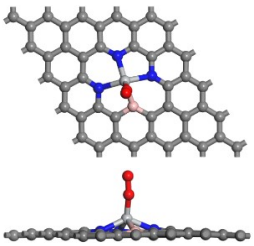	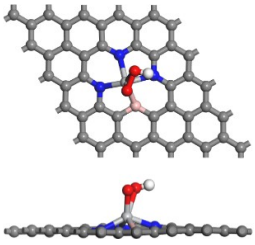	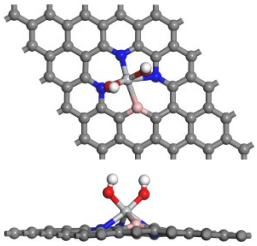
VN_3B	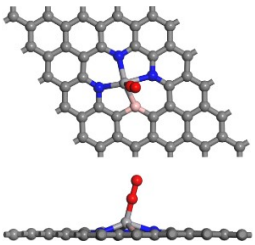	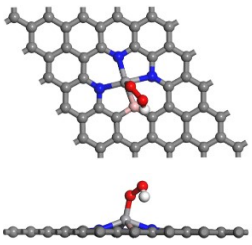	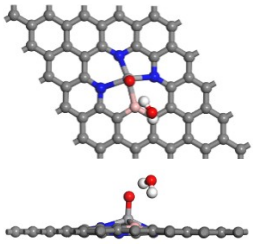
MnN_3B	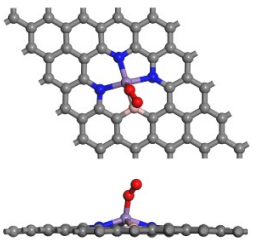	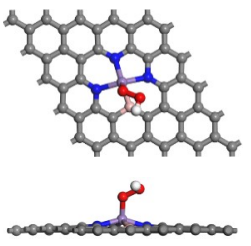	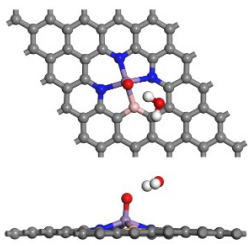
FeN_3B	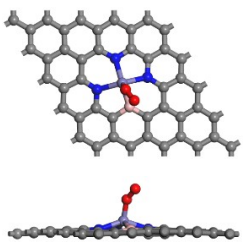	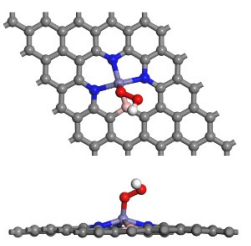	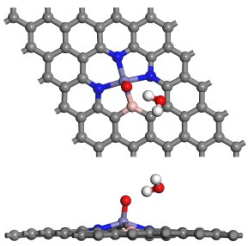
CoN_3B	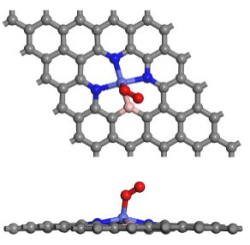	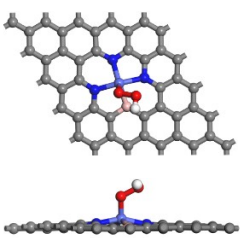	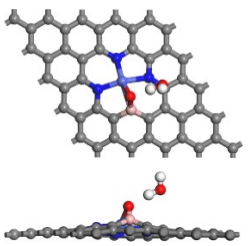

NiN_3B	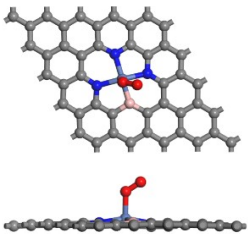	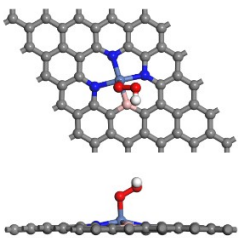	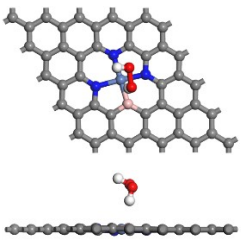
CuN_3B	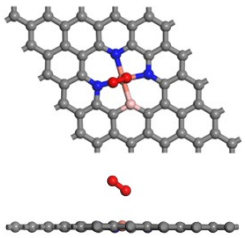		
ZnN_3B	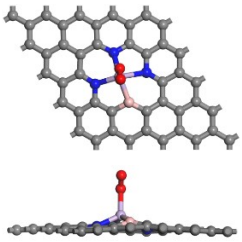	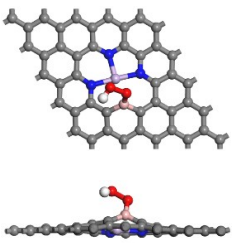	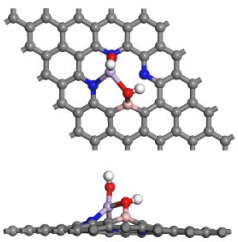
YN_3B	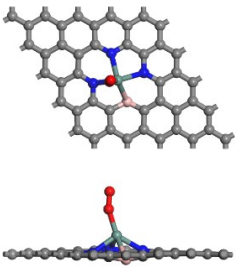	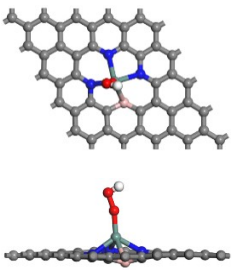	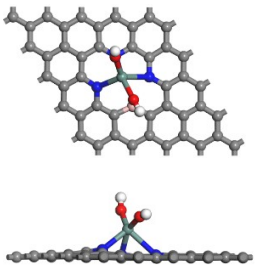
ZrN_3B	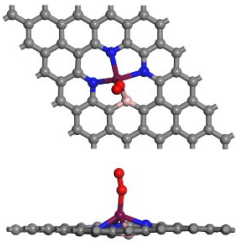	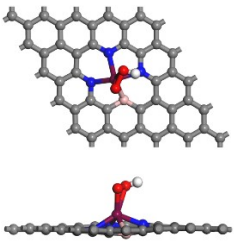	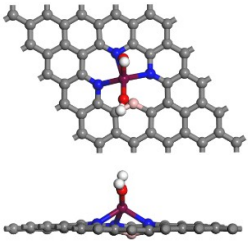
PdN_3B	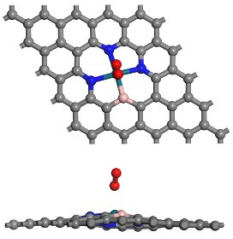		
HfN3B	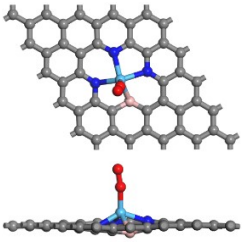	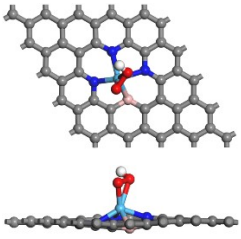	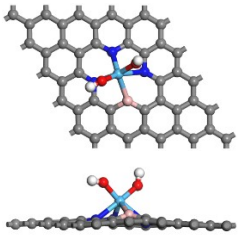

PtN3B	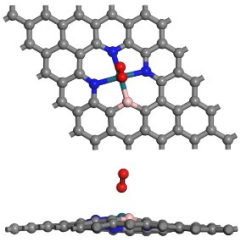

MN_2B_2-h	O_2*	OOH*	H_2O_2*
ScN_2B_2-h	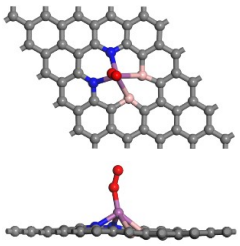	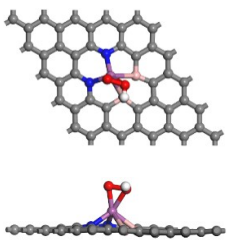	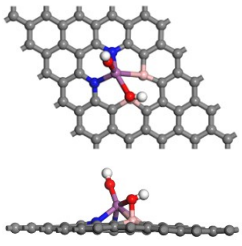
TiN_2B_2-h	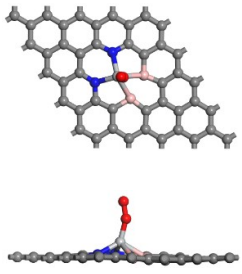	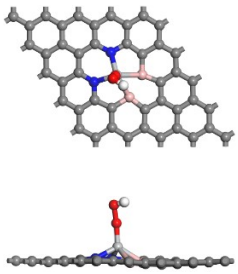	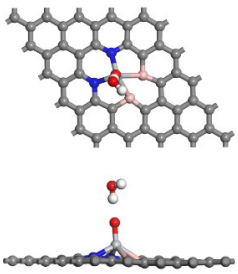
VN_2B_2-h	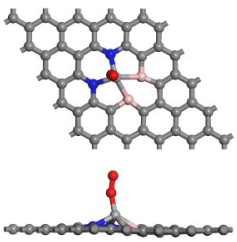	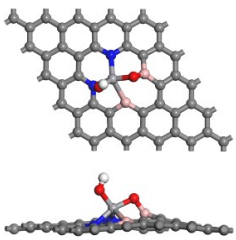	
CrN_2B_2-h	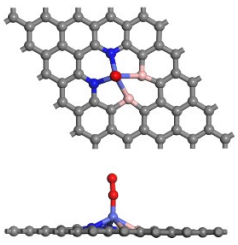	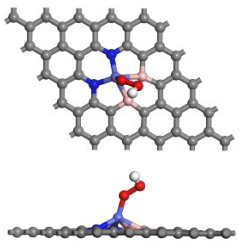	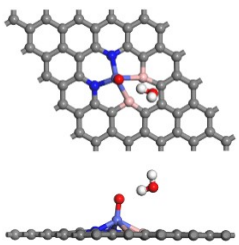
MnN_2B_2-h	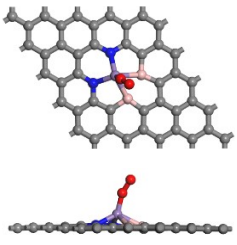	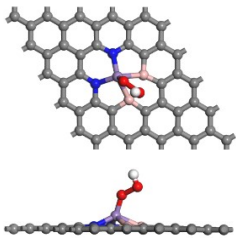	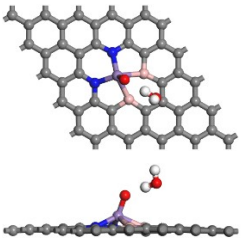

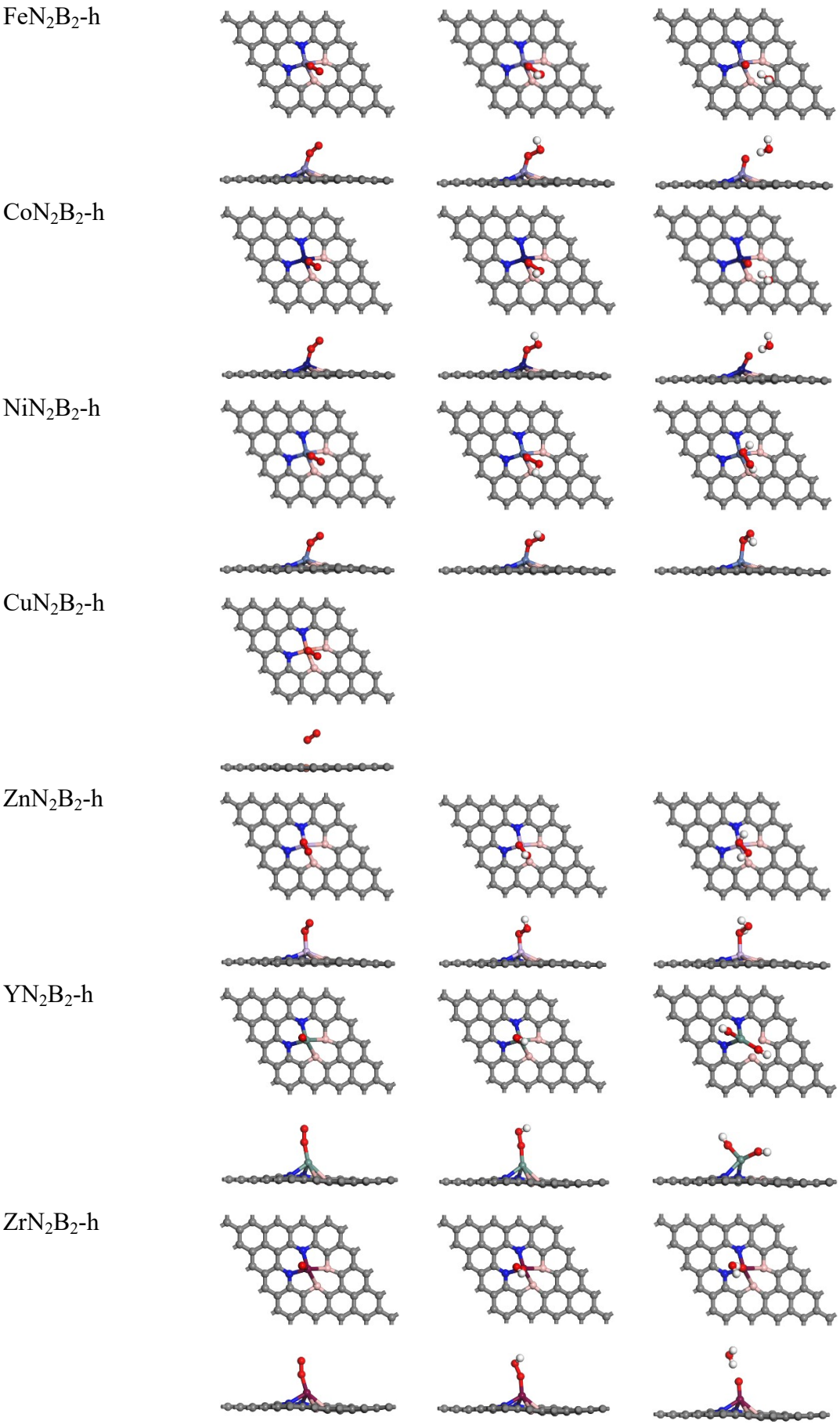
FeN_2B_2-h
CoN_2B_2-h
NiN_2B_2-h
CuN_2B_2-h
ZnN_2B_2-h
YN_2B_2-h
ZrN_2B_2-h

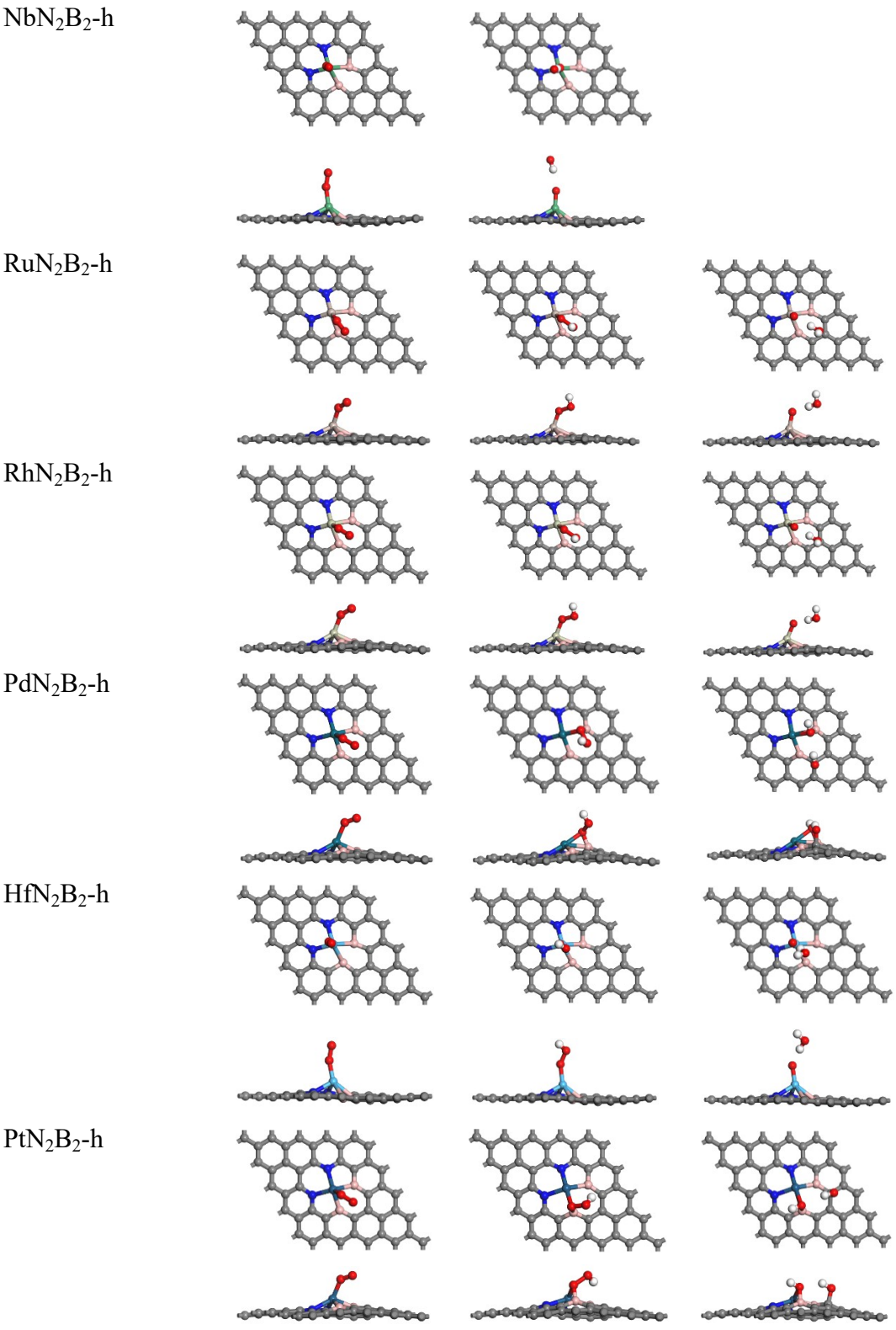
NbN_2B_2-h
RuN_2B_2-h
RhN_2B_2-h
PdN_2B_2-h
HfN_2B_2-h
PtN_2B_2-h

AuN_2B_2-h	

MN_2B_2-p	O_2*	OOH*	H_2O_2*
ScN_2B_2-p			
YN_2B_2-p			

MN_2B_2-o	O_2*	OOH*	H_2O_2*
NiN_2B_2-o			
PdN_2B_2-o			
PtN_2B_2-o			

MNB_3	O_2*	OOH*	H_2O_2*
$ScNB_3$	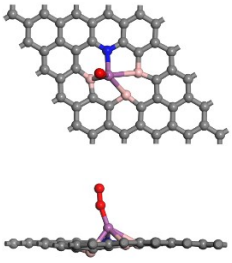	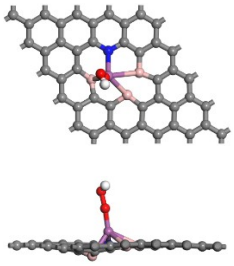	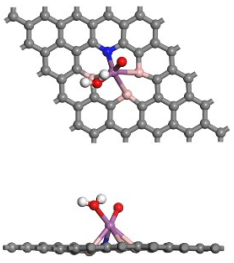
$NiNB_3$	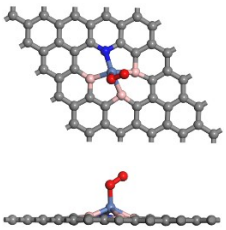	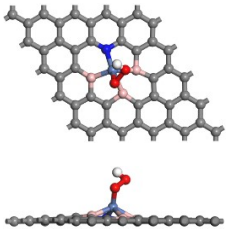	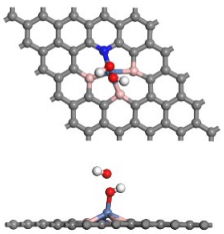
$PtNB_3$	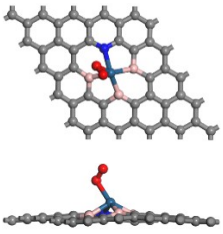	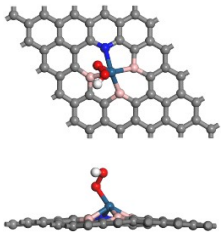	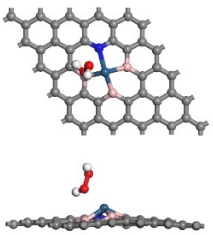
YNB_3	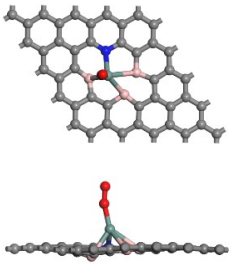	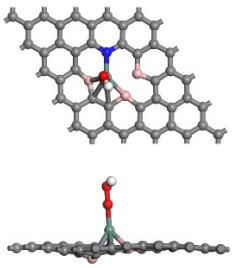	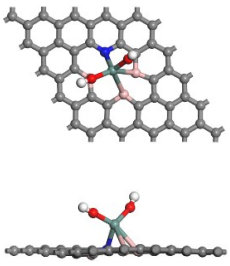

MB_4	O_2*	OOH*	H_2O_2*
ScB_4	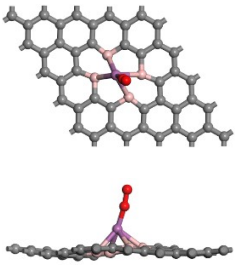	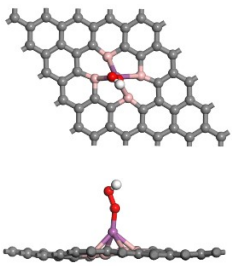	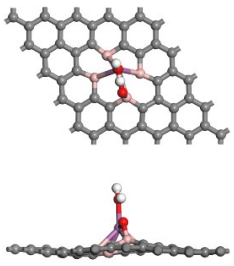
NiB_4	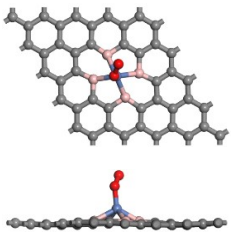	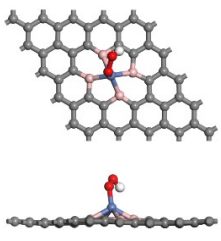	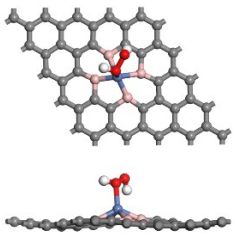

YB_4	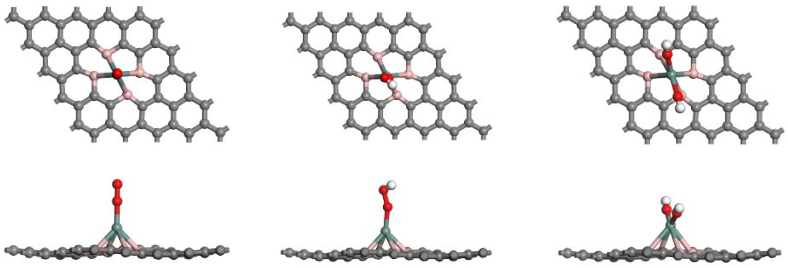		
RhB_4	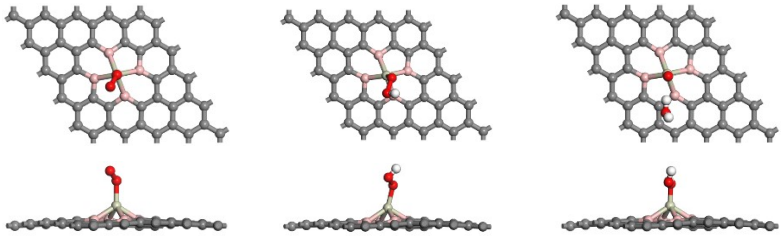		
PdB_4	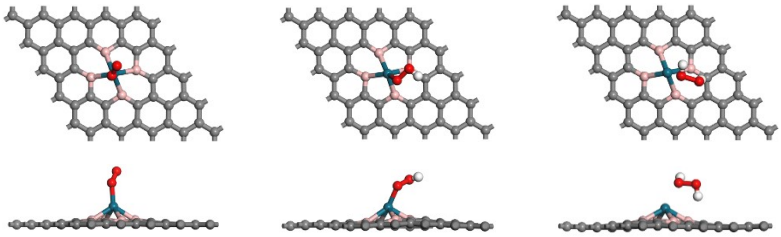		
PtB_4	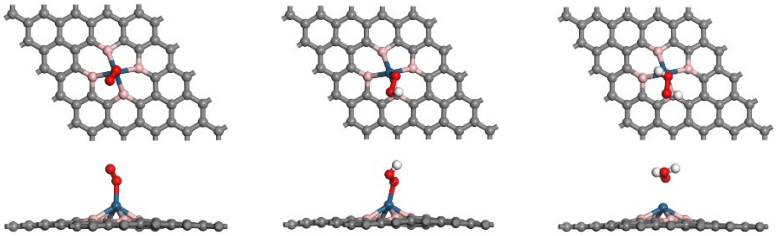		

Table S3. Adsorption energies of O_2 on various kinds of MN_xB_y.

Metal	E_{ads} (O_2, eV)					
	MN_3B	MN_2B_2-h	MN_2B_2-p	MN_2B_2-o	MNB_3	MB_4
Sc	-1.81	-1.98	-1.83		-1.77	-1.93
Ti	-2.12	-2.53				
V	-2.55	-2.88				
Cr		-2.16				
Mn	-1.60	-1.82				
Fe	-1.77	-1.68				

Co	-1.36	-1.65				
Ni	-0.46	-0.91		-0.67	-0.71	-0.90
Zn	-0.36	-0.45				
Y	-1.17	-1.95	-1.65		-1.83	-1.86
Zr	-2.05	-2.68				
Nb		-2.83				
Ru		-1.54				
Rh		-1.81				-0.92
Pd		-1.07				-0.50
Hf	-2.30	-2.96				
Pt		-1.18			-0.40	-0.65

Table S4. Adsorption energies of OOH on various kinds of MN_xB_y.

	E_{ads} (OOH, eV)					
Metal	MN_3B	MN_2B_2-h	MN_2B_2-p	MN_2B_2-o	MNB_3	MB_4
Sc	-3.15	-3.90	-3.20		-3.11	-3.41
Ti	-3.62	-3.53				
V	-3.52					
Cr		-3.97				
Mn	-2.42	-2.67				
Fe	-2.39	-3.73				
Co	-2.18	-2.28				
Ni	-1.15	-1.60		-1.64	-1.56	-1.81
Zn	-3.23	-1.35				
Y	-3.26	-3.37	-3.11		-3.34	-3.33
Zr	-3.62	-4.11				
Nb		-4.05				
Ru		-2.89				
Rh		-2.72				-2.11
Pd		-2.72				-1.82
Hf	-3.87	-4.21				
Pt		-2.61			-1.29	-2.02

Table S5. Adsorption energies of H_2O_2 on various kinds of MN_xB_y.

Catalyst	NiN_2B_2-h	ZnN_2B_2-h	NiB_4
E_{ads} (H_2O_2, eV)	-0.57	-0.47	-0.75

Table S6. Computed zero-point energy (*ZPE*), entropy correction (*TS*), Gibbs free energies of OOH* (ΔG_{OOH*}) and limited potentials (U_L) on catalyst surfaces. All free energies are computed relative to H_2O (l) and H_2 (g). The temperature is set to 298.15

K.

Catalyst	*ZPE* (eV)	*TS* (eV)	ΔG_{OOH*} (eV)	U_L (V)
NiN_3B	0.43	0.22	4.56	0.36
NiN_2B_2-h	0.43	0.22	4.10	0.58
ZnN_2B_2-h	0.43	0.21	4.36	0.56
$PtNB_3$	0.43	0.20	4.44	0.48
NiB_4	0.44	0.14	3.98	0.46
PdB_4	0.44	0.22	3.90	0.38
PtB_4	0.44	0.21	3.71	0.19

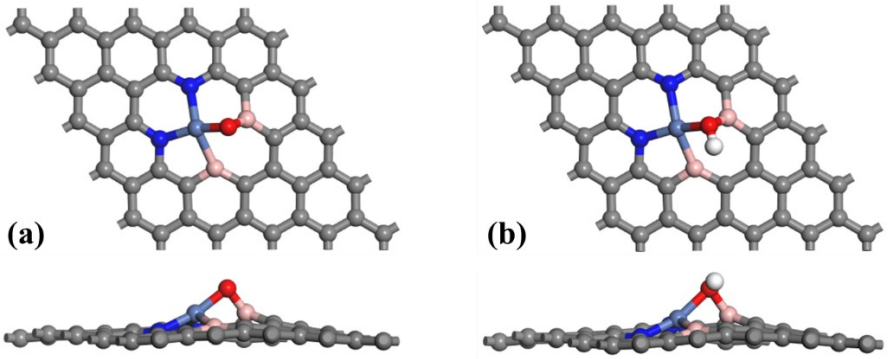

Fig. S3 Adsorption configurations of O* and OH* on NiN_2B_2-h.

Table S7. Computed zero-point energy (*ZPE*), entropy correction (*TS*) and Gibbs free energies (ΔG) of O* and OH* on NiN_2B_2-h. All free energies are computed relative to H_2O (l) and H_2 (g). The temperature is set to 298.15 K.

Adsorbates	*ZPE* (eV)	*TS* (eV)	ΔG (eV)
O*	0.10	0.03	0.32
OH*	0.42	0.04	0.14

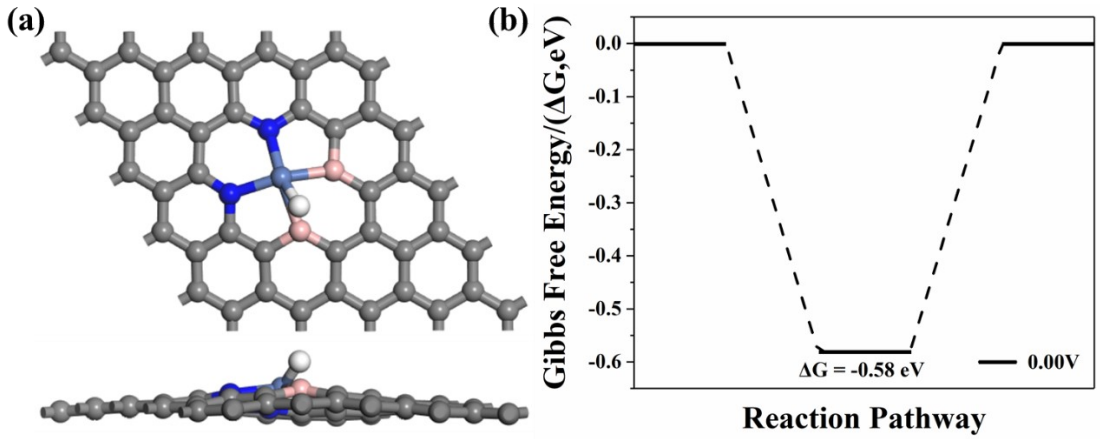

Fig. S4 Adsorption configuration of H* and Gibbs free energy diagram for HER on

NiN_2B_2-h at U = 0 V.

Table S8. Computed zero-point energy (ZPE), entropy correction (TS) and Gibbs free energy (ΔG) of H* on NiN_2B_2-h. All free energies are computed relative to H_2O (l) and H_2 (g). The temperature is set to 298.15 K.

Adsorbates	*ZPE* (eV)	*TS* (eV)	ΔG (eV)
H*	0.24	0.01	-0.58

Table S9. Parameters for NiN_4, NiN_2B_2-h, O_2*, OOH* and H_2O_2* on NiN_2B_2-h: bond lengths, bond angles. The N-Ni-N bond angle of NiN_4 is in the hexatomic ring.

	Bond length (Å)				Bond angle (degree)	
Species	Ni-O	O-O	Ni-B	Ni-N	B-Ni-B	N-Ni-N
NiN_4				1.88		88.08
NiN_2B_2-h			2.00	1.89	66.86	90.00
O_2*	1.75	1.28	2.07	1.98	69.72	84.93
OOH*	1.79	1.44	2.07	1.94	64.05	85.85
H_2O_2*	2.13	1.48	2.03	1.92	64.66	87.94

Table S10. Activation barrier (ΔE_a) for each elementary step of H_2O_2 formation and side actions on NiN_2B_2-h.

Reaction Pathway	Activation Barriers (E_a, eV)
$O_2^* \rightarrow 2O^*$	0.82
$O_2^* + H^* \rightarrow OOH^*$	0.22
$OOH^* \rightarrow O^* + OH^*$	1.13
$OOH^* + H^* \rightarrow O^* + H_2O$	1.57
$OOH^* + H^* \rightarrow H_2O_2^*$	0.45
$H_2O_2^* \rightarrow 2OH^*$	0.51
$H_2O_2^* \rightarrow H_2O_2 + *$	0.42
$H_2O_2^* + H^* \rightarrow OH^* + H_2O$	2.34

O* + H* → OH*	0.73
OH* + H* → H_2O*	2.44
H_2O* → H_2O + *	0.31

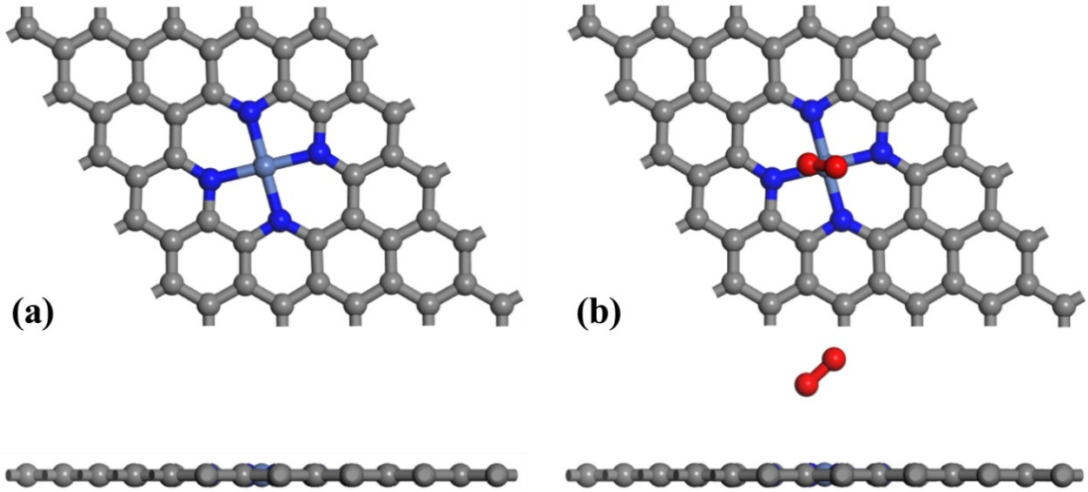

Fig. S5 Optimized structures of NiN_4 and O_2 adsorption on NiN_4.

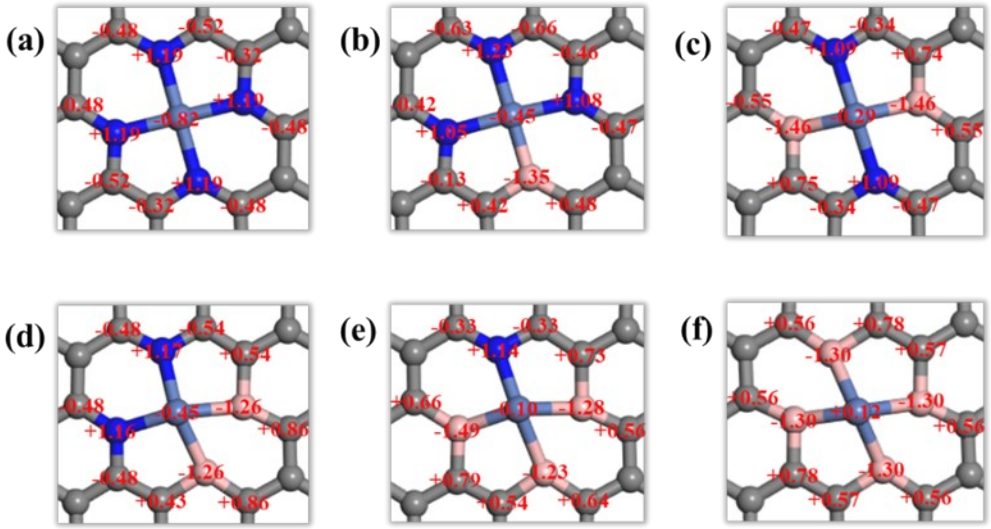

Fig. S6 Bader charge analysis of NiN_4 and NiN_xB_y. The "+" and "-" represent gaining and losing electrons, respectively.

Table S11. Bader charge analysis of Ni atoms and O atoms connected with Ni in O_2*, OOH* species on NiN_xB_y and NiN_4. The "+" and "-" represent gaining and losing electrons, respectively.

Catalyst	Q (Ni, e)	Q (O_2, e)	Q (OOH, e)	E_{ads} (O_2, eV)

NiN_3B	-0.45	+0.36	+0.4	-0.45
NiN_2B_2-h	-0.45	+0.39	+0.39	-0.91
NiN_2B_2-o	-0.29	+0.38	+0.46	-0.67
$NiNB_3$	-0.1	+0.38	+0.45	-0.71
NiB_4	+0.12	+0.40	+0.34	-0.91
NiN_4	-0.82			

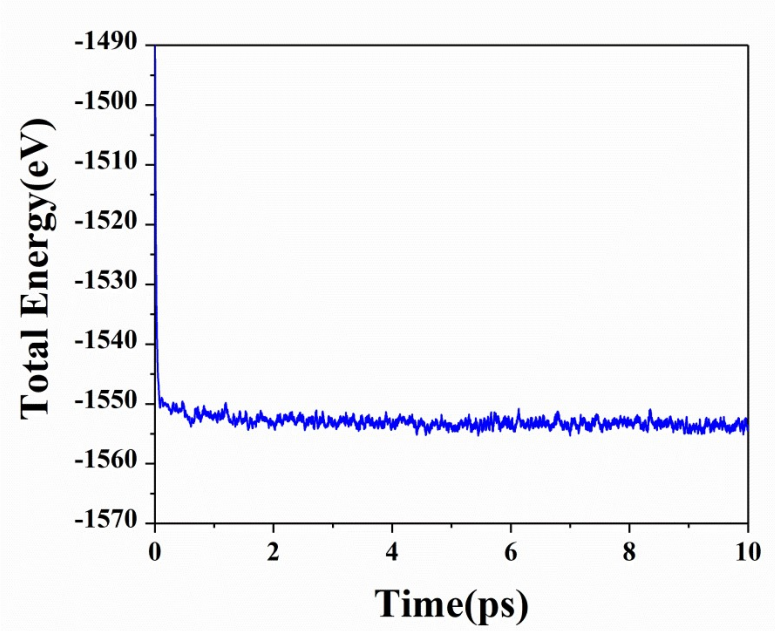

Fig. S7 The total energy change of NiN_2B_2-h under 0.5M H_2SO_4 solution after 10 ps AIMD simulation at 298.15 K.

Table S12. Bond lengths for O_2*, OOH* and H_2O_2* on the NiN_2B_2-h in gas and SO_4^{2-}

anion solution, respectively. The Ni-O represents the O atoms bonded with Ni.

	Bond length in gas		Bond length in SO_4^{2-} anion solution		E_{ads} (eV)	
Adsorbates	Ni-O (Å)	O-O (Å)	Ni-O (Å)	O-O (Å)	gas	solution
O_2*	1.75	1.28	1.91	1.31	-0.91	-0.88
OOH*	1.79	1.44	1.88	1.43	-1.61	-1.61
H_2O_2*	2.13	1.48	2.10	1.46	-0.57	-1.20

Table S13. Activation barrier (ΔE_a) for each elementary step of H_2O_2 formation and side actions on NiN_2B_2-h under SO_4^{2-} anion solution.

Reaction Pathway	Activation Barriers(eV)
$O_2^* \rightarrow 2O^*$	2.60
$O_2^* + HSO_4^- \rightarrow OOH^* + SO_4^{2-}$	0.57
$OOH^* \rightarrow O^* + OH^*$	1.39
$OOH^* + H^* \rightarrow O^* + H_2O$	1.06
$OOH^* + H^* \rightarrow H_2O_2^*$	0.15
$H_2O_2^* \rightarrow 2OH^*$	1.28
$H_2O_2^* \rightarrow H_2O_2 + *$	0.63
$H_2O_2^* + H^* \rightarrow OH^* + H_2O$	3.00

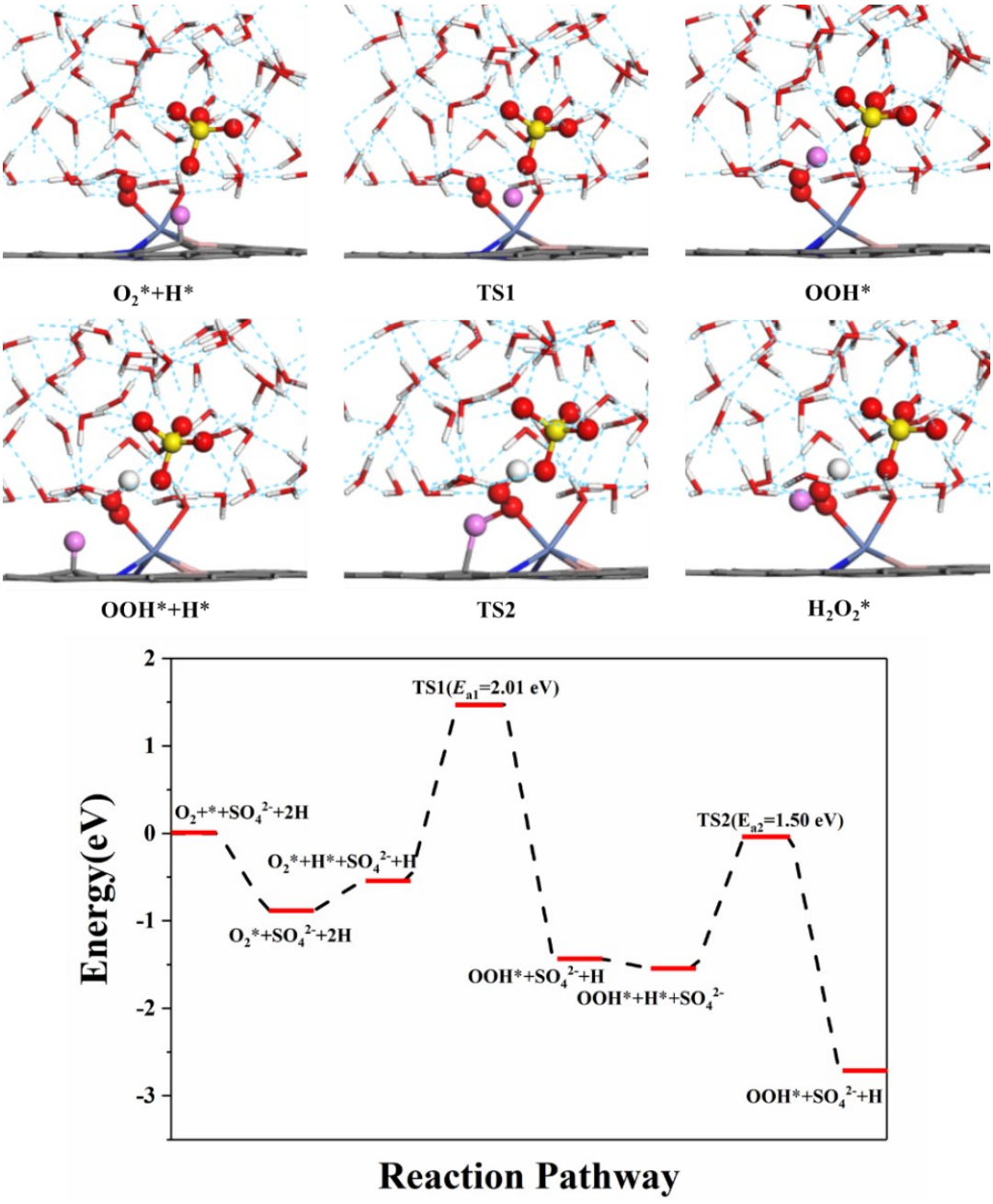

Fig. S8 Energy and profile of optimized structures for the O_2 hydrogenation to H_2O_2* on NiN_2B_2-h under SO_4^{2-} anion solution. The H atoms are gained from support directly. Color code: C, brown; Ni, navyblue; O, red; N, blue; B, pink; S, yellow; H, white; transferred H, magenta.

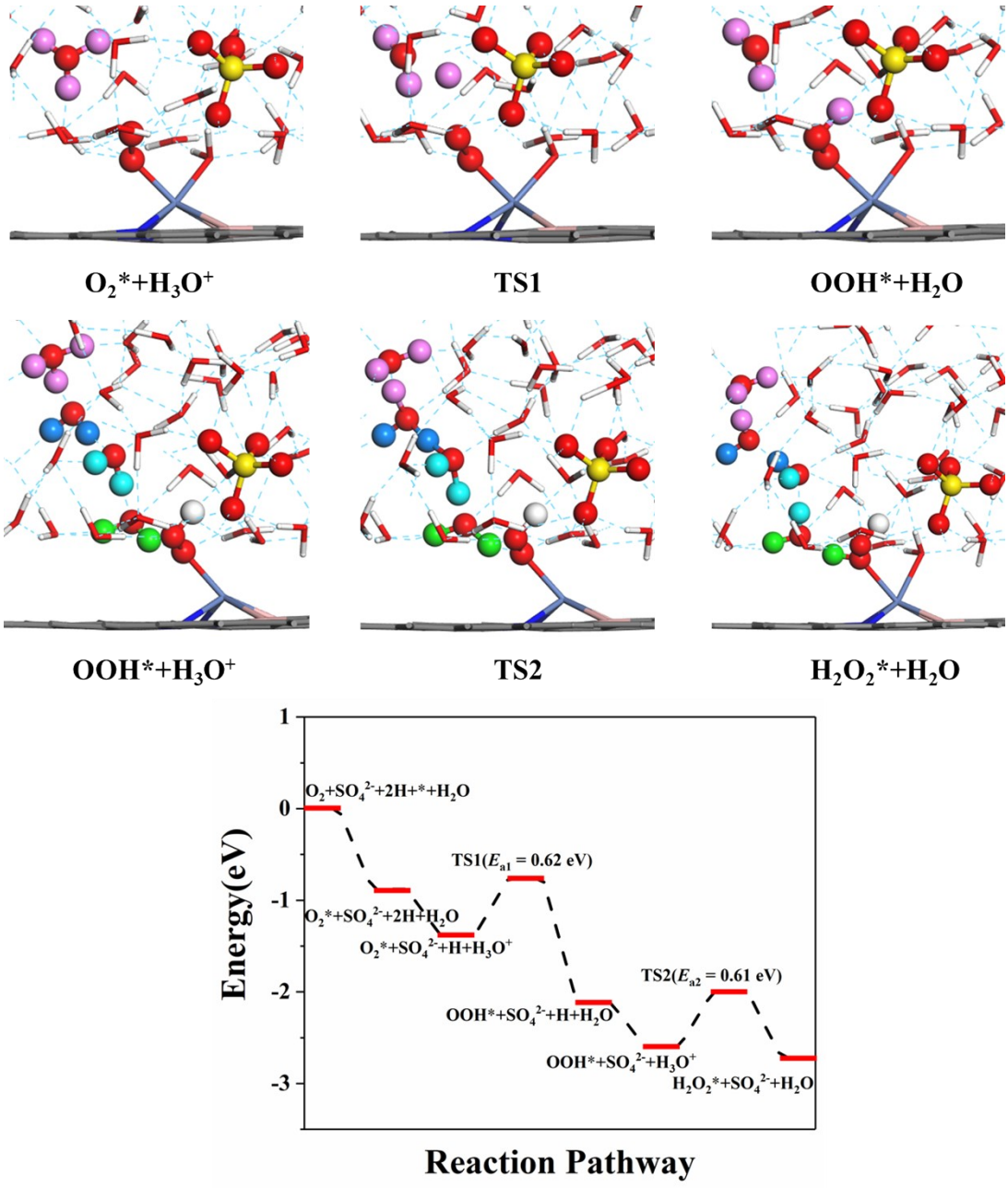

Fig. S9 Energy and profile of optimized structures for the O_2 hydrogenation to H_2O_2* on NiN_2B_2-h under SO_4^{2-} anion solution. The H atoms are gained from H_3O^+. Color code: C, brown; Ni, navyblue; O, red; N, blue; B, pink; S, yellow; H, white; transferred H, magenta, dodger blue, cyan and green.